Atmospheric Research 294 (2023) 106980

Contents lists available at ScienceDirect

Atmospheric Research

journal homepage: www.elsevier.com/locate/atmosres

Changes in the mechanism of the South-Asian summer monsoon onset propagation induced by the pre-monsoon aerosol dust storm

Soumik Ghosh [a,1], Abhijit Sarkar [b], R. Bhatla [a,c], R.K. Mall [c,d], Swagata Payra [e,*], Priyanshu Gupta [d]

[a] Department of Geophysics, Institute of Science, Banaras Hindu University, Varanasi, India
[b] National Centre for Medium Range Weather Forecasting, Noida, UP, India
[c] DST-MCECCR, IESD, Banaras Hindu University, Varanasi, India
[d] IESD, Banaras Hindu University, Varanasi, India
[e] Department of Remote Sensing, Birla Institute of Technology Mesra, Ranchi, Jharkhand, India

ARTICLE INFO

Keywords:
Indian summer monsoon (ISM)
ISM Onset and advance
Aerosol Optical Depth (AOD)
Dust storm
REGional climate Model v4.7 (RegCM4.7)
Elevated heat pump

ABSTRACT

A modeling effort is considered to understand the effect of dust aerosol storms in the Indian summer monsoon (ISM) onset propagation over the Indian subcontinent. The study found how the dust aerosol loading during the pre-monsoon period over the Indian subcontinent positively impacts the advancing ISM onset. The heavy loading of dust aerosol from middle east Asia to the northwest (NW) Indian region boosts the temperature gradient over the mid-troposphere. This sudden rise in the mid-tropospheric atmospheric temperature triggers the low-pressure belt over the monsoon trough. It amplifies the Elevated Heat Pump mechanism and loads enough dust for the dust storm over north India. The formation of the monsoon trough over the Indo-Gangetic Plain (IGP) pulls the moisture-loaded wind towards the Indian subcontinent and the IGP, followed by the onset of monsoon over Kerala within a week. Due to this storm, the intense heat gradient in the troposphere also induces the monsoon propagation and the monsoon advancement from Kerala to BoB within a short time. However, it makes up for the naturally delayed monsoon on time.

Plain language summary: Study shows how the pre-monsoon dust storm modulates the Indian summer monsoon (ISM) propagation over the Indian region. The onset of the monsoon was delayed in a particular year, and the pre-monsoon dust storm over northwest India changed the regular monsoon mechanism and generated an entirely different mechanism. The elevated heat pump theory applies that pushes the monsoon advancement faster than usual. A dust storm over north India causes a sudden rise in the mid-tropospheric temperature gradient and more rapid monsoon advancement than usual.

1. Introduction

The World's most prominent and complicated monsoon system is the Indian monsoon. It is a gigantic phenomenon that controls the water cycle and the country's economy. Recent studies show its changing pattern in response to climate change, and the Monsoon researcher are doing their best to investigate and understand this complicated system. The CMIP intra-model variability shows the changes in the seasonal monsoon rainfall over the different regions of India (e.g., Parth Sarthi et al., 2015; Parth Sarthi et al., 2016; Shahi et al., 2021) and the South Asia region (e.g., Bollasina et al., 2011; Ganguly et al., 2012). Climate change also affects the climate and weather extreme events over the Indian subcontinent and changes the climate dynamics over small and large scales (Ongoma and Tabari, 2023). Considering these climatic conditions, it is essential to understand the underlying mechanism for reliable weather prediction.

Several studies have been carried out to understand the Indian summer monsoon (ISM) variability at the regional scale. Bhatla et al. (2016), Maharana and Dimri (2016), and Ghosh et al. (2019); Ghosh et al. (2022) have investigated the intraseasonal monsoon variability using the RegCM and successfully explained the model capacity in simulating the different epochs of monsoon and the associated monsoon

* Corresponding author.
E-mail addresses: soumik.ghosh@fulbrightmail.org (S. Ghosh), spayra@gmail.com (S. Payra).
[1] Present Affiliation: Department of Earth and Planetary Sciences, Weizmann Institute of Science, Rehovot, Israel.

https://doi.org/10.1016/j.atmosres.2023.106980
Received 3 February 2023; Received in revised form 12 August 2023; Accepted 26 August 2023
Available online 29 August 2023
0169-8095/

dynamics behind it. This downscaled regional model is further used to describe the role of Arabian Sea warming in the ISM (Mishra et al., 2020a). Ghosh et al. (2023) have diagnosed the presence of the northward propagating monsoon oscillation and the monsoon intraseasonal oscillation using the updated version of the RegCM that Ghosh et al. (2022) used to explain the intraseasonal monsoon variability over the Indian region. Further, Bhatla et al. (2020) have studied the intraseasonal monsoon variability over the homogeneous monsoon region using the same model and investigated an extensive modeling study on modulating summer monsoon rainfall variability in the variation of drought and flood events (Verma et al., 2022). Verma et al. (2021) and Sinha et al. (2013) further studied the model's sensitivity by focusing on model parameterization. A connection between the teleconnection and the monsoon variability over the homogeneous region of India has also been established (Verma and Bhatla, 2021). A study also noted when the RegCM model simulates rainfall extremes over a specific region (Pant et al., 2022), further focused on the monsoon extremes using extensive statistical methods and explained the model's suitability to study the monsoon extremes (Mishra and Dubey, 2021; Pant et al., 2023).

Studies found that the ISM is very much influenced over the ocean and land region by aerosol. Many scientific studies documented the inter-annual and intra-seasonal variability of ISM rainfall that can be affected by an increase in absorbing aerosol concentrations, especially carbonaceous aerosols and desert dust (Meehl et al., 2008; Bollasina et al., 2011; Ganguly et al., 2012; Solmon et al., 2015; Das et al., 2016; Maharana et al., 2019). Aerosol directly scatters and absorbs the incoming solar radiation and indirectly influences various atmospheric phenomena like cloud albedo, cloud formation, cloud lifetime, and probability of precipitation by altering the size and density of cloud droplets (Lohmann and Feichter, 2005; Kosmopoulos et al., 2008; Papadimas et al., 2008). At different levels, an aerosol effect on cloud microphysical properties causes both suppressions and invigoration of precipitation and affects the diurnal cycle and global monsoon patterns (Stocker, 2014). It happens by changing the cloud droplet's size distribution, precipitable water redistributions, condensation, and evaporation derived from latent heat changes.

The possible impact of aerosol on monsoon circulation depends on the types of anthropogenic aerosols. Anthropogenic and natural aerosols (e.g., sea salt and mineral dust) cause the spatiotemporal variability of aerosol optical depth (AOD), which depends on topography, season, local atmospheric process, and aerosol radiative feedback (Nober et al., 2003; Koren et al., 2012). Jiang et al. (2013) observed that sulfates and primary organic matter suppress precipitation over north China compared with anthropogenic black carbon (BC) species. The study is further supported by Das et al. (2016); they reveal the weakening effect of BC, organic carbon (OC), and Sulfur Dioxide (SO2) on ISM, due to which the surface pressure over the landmass is increased that obstructs the south-west monsoon wind flow. It is found that the local and long-range transported aerosols are responsible for the precipitation (Ganguly et al., 2012). Combined effects of microphysical and dynamical impacts of aerosol radiative forcing interlaced with the meteorological forcing complicate the aerosol-monsoon connection at various space and time scales (Das et al., 2016). The role of absorbing aerosols during the pre-monsoon season and their indirect role during ISM breaks are briefly studied by Jin et al. (2021). Manoj et al. (2011) studied the interaction of aerosol-cloud during two break spells for a particular year. They have reported that the aerosol indirectly suppresses the precipitation in central India.

Lau et al. (2006) hypothesized the elevated heat pump theory which explained that atmospheric heating is due to elevated aerosols from anthropogenic and natural sources that lead to changes in the monsoon life cycle derived from the increased rainfall and advancement of monsoon rainfall. Vinoj et al. (2014) have studied the strengthening of ISM circulation ascribed to a large-scale convergence induced by dust over the Arabian Peninsula. The weakening of monsoon circulation due to enormous aerosol loading is observed by Ramanathan et al. (2005). They explained that the solar dimming effects, due to which the aerosol may cause north-south thermal contrast reduction, consequently suppressing the ISM rainfall. Solar dimming over central and northern India cools the surface air more than the air above it, which impedes convection (Lau et al., 2006). Meehl et al. (2008) have reported an increase in the meridional tropospheric temperature gradient between the Tibetan Plateau and the southern area and increased precipitation over the Indian region that BC aerosols may induce. However, several studies have focused on the aerosol-precipitation interaction and their relationship. Due to complex mechanisms and regional scale variability in aerosol distribution, it is still a part of the uncertainty. By increasing the cloud condensation nuclei, the heavy aerosol loads may decrease the number of monsoon depressions (Krishnamurti et al., 2013). The observed and satellite measurements are suitable for explaining this microphysical link between aerosols and cloud properties (Heymsfield and McFarquhar, 2001; Konwar et al., 2012). But climate models perform well in simulating the capabilities of the aerosol and meteorological parameters that emerge in understanding the dynamic relationship between aerosol and cloud interaction. High-resolution dynamical downscaling of the RegCM can better simulate atmospheric aerosol distribution and circulation. Several studies have emphasized the aerosol and ISM interaction using RegCM (Das et al., 2016; Solmon et al., 2015; Maharana et al., 2019). For example, natural and anthropogenic aerosols are studied using the RegCM4 model with an aerosol module by Zakey et al. (2006) and Solmon et al. (2006). However, to research dust transport over the Indian Subcontinent, Das et al. (2013) used RegCM with dust aerosol forcing (0.01–20 μm). Nair et al. (2012) performed the simulation of anthropogenic aerosol by using RegCM and found that a factor of 2–5 underestimates the BC concentration concerning in-situ measurements. The sensitivity of monsoon circulations to dust absorption using RegCM4 is briefly described by (Das et al., 2016), while another study by Solmon et al. (2015) found that the radiative dust forcing induces a critical dynamical feedback which may lead to the regional moisture convergence and precipitation over Southern India during ISM season.

The relation between the ISM rainfall (ISMR) variability and the Aerosol is well-established and well-accepted by climate researchers. However, the challenges the monsoon rainfall prediction and propagation due to the aerosol are well documented by Jin et al. (2021), which further seek some critical attention in describing the propagation of monsoon epochs like monsoon onset and the role of pre-monsoon aerosol dust over the subcontinent in there is any changes in the monsoon mechanism. Furthermore, the climate model seeks more consideration to improve simulation, and including aerosol/dust in the model is one of those. Therefore, our primary objective is to examine the ISM rainfall (ISMR) scenario if the climate model considers the real dust load for the realistic simulation because the possible relationship and the dynamics behind the monsoon propagation induced by the dust aerosol The study considered the regional climate model simulation confirming the dust module for a realistic simulation and establishing the possible dynamics behind the monsoon onset propagation induced by the dust aerosol.

2. Data and methodology

2.1. Model physics and experiment design

The latest development of the Abdus Salam International Centre for Theoretical Physics (ICTP) regional climate model, RegCM version-4.7 (RegCM4.7), is used to carry out this study. The Sigma vertical coordinate system is followed for the terrain. The mesoscale model (MM5) (Grell et al., 1994) is used as a hydrostatic dynamical core where the model cells are on Arakawa B-grid. More information can be found in Elguindi et al. (2013) and Giorgi et al. (2012). This hydrostatic version of the model has multiple physics parameterization options. It offers to choose a parameterization scheme specifically over land and ocean

regions based on the study requirement over different Co-Ordinated Regional Climate Downscaling EXperiment (CORDEX) domains (e.g., Giorgi et al., 2012). The physics of the radiation parameterization is considered using the CCM3 radiation scheme (Kiehl et al., 1996), and the parameterization scheme is regarded as a mixed scheme mode over South Asia (SA) CORDEX. The combination of the mixed type cumulus schemes successfully tested at the ICTP for the SA-CORDEX, where the MIT scheme (Emanuel and Živković-Rothman, 1999) is used over land, and the Tiedtke scheme (Tiedtke, 1989) is considered over the ocean. The ocean flux parameterization scheme follows Zeng et al. (1998). The land surface scheme of Community Land Model version 4.5 (CLM4.5) (Oleson et al., 2013) and UW boundary layer scheme (Bretherton et al., 2004) is used. The large-scale precipitation in the model is explained using the Subgrid Explicit Moisture Scheme (SUBEX) scheme (Pal et al., 2000).

The model run is set up at a horizontal resolution of 25 km over the SA-CORDEX domain with 23 vertical levels. The highest level of the model simulation is set at 50 hPa, and the domain with (13°N, 70°E) as the center. The initial and boundary condition (ICBC) and sea surface temperature (SST) are obtained from 6 h of EIN75 datasets (Dee et al., 2011). The United States Geological Survey (USGS) topography and land use data are considered at 30″. The rotated Mercator map projection is used. The time step of model integration is 30 s. The aerosol feedback to the atmosphere is activated, and the dust module with 04 bins is considered for this simulation. The model is integrated on hourly time from 24*th* May 2014 to 30*th* June 2014, where the initial three days are regarded as spin-up time and therefore are excluded from the analysis. The aerosol feedback to the atmosphere is activated to see the aerosol impact on climate.

2.2. Methodology

The model experiment is set up over the SA-CORDEX region Fig. 1, and the model data validation is considered over the SA-CORDEX region. Several analyses are carried out over the IGP region to meet the proposed objectives. The capital of India, Delhi, and its surrounding region faced massive dust storms on May 30*th*, 2014. The geographical location of Delhi (77.10°E, 28.70°N) comes under the active aerosol region and faces aerosol-related problems regularly. This massive metropolitan area is spread over 1484 km^{-2} (approximately 1.5°) and accommodates 1.9 crores of people per the 2012 census. Therefore, 26–30°N and 76–80°E are considered to cover the metropolitan area domain and meet the research goal. The area of Delhi comes under the Indo-Gangetic Plain (IGP) region (top right of Fig. 1), is the most aerosol-prone area, and is considered to carry out the aerosol load concentration over the Indian region. Along with it, the IGP region is known to significantly impact the Indian monsoon regarding the monsoon trough distribution and advance of monsoon rainfall over India. Model simulated rainfall is validated using the ERA5 rainfall (Hersbach et al., 2020) from May 27*th* to June 30*th*, 2014. The rainfall distribution for the specific days is compared with the Tropical Rainfall Measuring Mission (TRMM) rainfall. The area-averaged Global Precipitation Climatology Project (GPCP) daily satellite rainfall is interpolated to generate hourly time steps and considered to measure rainfall over Delhi before and after of dust storm. However, the model simulated AOD distribution on May 30*th*, 2014, is validated using the Moderate Resolution Imaging Spectroradiometer (MODIS) satellite data and is masked to the MODIS dataset to provide visual ease. The model simulated AOD is also validated with the Aerosol Robotic Network (AERONET) station AOD over Jaipur (Rajasthan state) and Kanpur (Uttar Pradesh state). AERONET station over Delhi was not functional up to that time, therefore, the station AOD over Delhi is absent for 2014, and the reason to consider the nearest station (Jaipur and Kanpur) for this study. To keep the consistency and to avoid the perturbed distribution by comparing the model performance using other reanalysis data, authors considered the ECMWF's dataset for the initial and lateral boundary forcing to RegCM4.7 and model validation. The correlation coefficient (CC), Bias, root mean square error (RMSE), mean absolute error (MAE), and fractional bias (FB) techniques are considered for the model validation. The synoptic pattern of the MSLP advancement over NW India is latitudinally and longitudinally centered at 27°N and 70°E to understand the propagation of MSLP during the considered period, respectively. The spatial data distribution has been signified using a student *t*-test with a 99% confidence level and superimposed with a hatch sign over the spatial pattern. The monsoon trough largely controls the rainfall over Kerala and the Bay of Bengal (BoB) and, therefore, the temporal pattern of rainfall distribution over those areas is considered over 70–80°E and 5–10°N, and 86–92°E and 18–23°N, respectively.

2.2.1. Mean absolute error (MAE)

The absolute error is the difference between the true value and the model simulated result and may represent as:

$$\Delta X = M_i - X \tag{1}$$

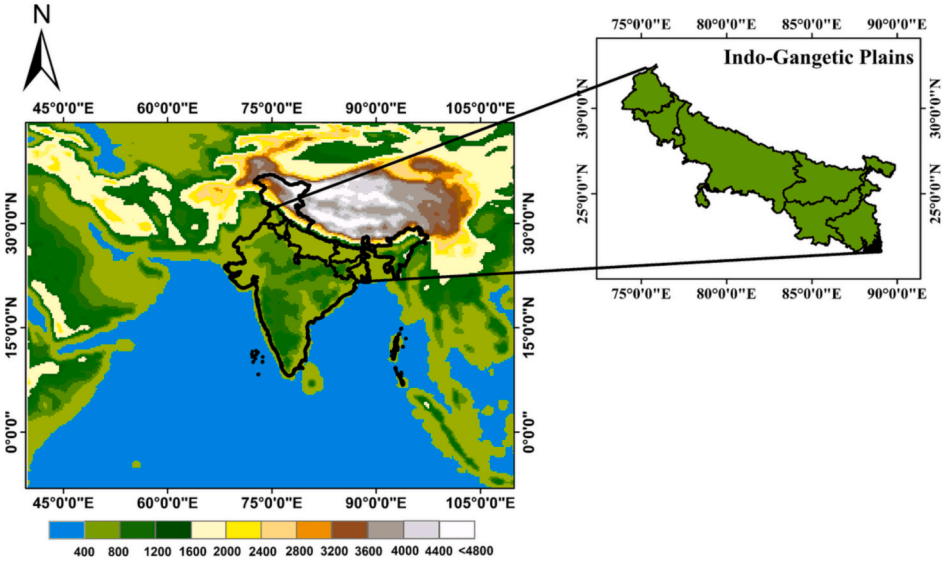

Fig. 1. Representation of the SA-CORDEX domain and the topography considered for the study. The extended area, denoted at the top right corner is the IGP considered for this study.

Where M_i stands for the simulated value at record i and X is the 'true' or 'observed' value. The long-time average of the absolute error is pointed as the Mean Absolute Error (MAE) and can be written as:

$$MAE = \frac{1}{n}\sum_{i=1}^{n}|M_i - X| \tag{2}$$

Where n = the number of absolute errors, $|M_i - X|$ is the absolute errors.

2.2.2. Fractional bias (FB)

The fractional bias is calculated as follows:

$$FB = \frac{1}{n}\left(\frac{\sum_1^n (M_i - X)}{\sum_1^n \left(\frac{M_i + X}{2}\right)}\right) \tag{3}$$

M_i stands for the simulated value at record i, and X is the 'true' or 'observed' value.

2.2.3. Root mean square error (RMSE)

The RMSE is calculated as: The fractional bias is calculated as follows:

$$RMSE = \sqrt{\frac{1}{n}\sum_{i=1}^{n}(M_i - X_i)^2} \tag{4}$$

M_i and X_i are the simulated value of record i and the observed value at record i, respectively.

3. Results and discussions

3.1. 2014 ISM onset and pre-monsoon dust storm

The gateway of the ISM over India region is Kerala. After the humid and hot summer in India, the monsoon hits Kerala after May 10*th* with the normal date of June 1*st*, and it takes another week to cover the BoB. Monsoon covers the whole country and reaches the highest point of Rajasthan by the normal date of July 8*th*. However, these monsoon propagation dates are normal, and actual dates depend upon the moist static energy (MSE) and heat gradient over the subcontinent. In the 2014 monsoon year, two days before the normal onset days, there was no rain over Kerala (Fig. 2a). That particular year, the monsoon onset was delayed by five days of the normal onset date. The midlatitude circulation regime makes favorable conditions for the passage of Western disturbances. It causes heat low over northern India and delayed onset over the Indian region for a particular year (IMD Met. Monograph 2014 Pai and Bhan, 2014). As per the report, the settings of monsoon onset formed at its normal position over west Pakistan and its surrounding region by June 6*th*, and the monsoon hit Kerala (Fig. 2b). The monsoon also advanced over the southwest BoB and some parts of west-central BoB on the same day. For the particular year, the onset advance from Kerala to BoB was much faster than its usual time, and the advancement of monsoon hit BoB on June 8*th*. It took only two days to cover the BoB this year. Afterward, within one and a half weeks, monsoon advanced over Bihar and Jharkhand and its surrounding region and made up for the delay. However, the question remains: Where did the monsoon get enough energy to advance over the entire BoB within a couple of days for the particular year? During the pre-monsoon, on 30*th* May 2014, just before two days of normal onset days, the IGP and the NW Indian region experienced a massive dust storm (Fig. 2c). Delhi was the epicenter of the dust storm (Chakravarty et al., 2021; Sethi et al., 2021). The atmosphere over the regions was hot before and during the dust event (Chakravarty et al., 2021). The Shortwave aerosol direct radiative forcing is found −10 W m^2, 27 W m^2, and − 37 W m^2 at the top of the atmosphere, the atmosphere, and surface, respectively, over that region and the heating rate was enhanced by 56% in the atmospheric column during that event (Sethi et al., 2021). This paper has attempted to investigate if there is any relationship between the aerosol dust storm and the Indian monsoon onset and its propagation.

3.2. Monsoon variability in RegCM4.7

The onset and the advance of monsoon solely depend on the ocean part regarding the rainfall propagation and source of moisture supported by the other synoptic mechanism over the land region. For this purpose, the rainfall pattern in the model simulation is validated for the entire

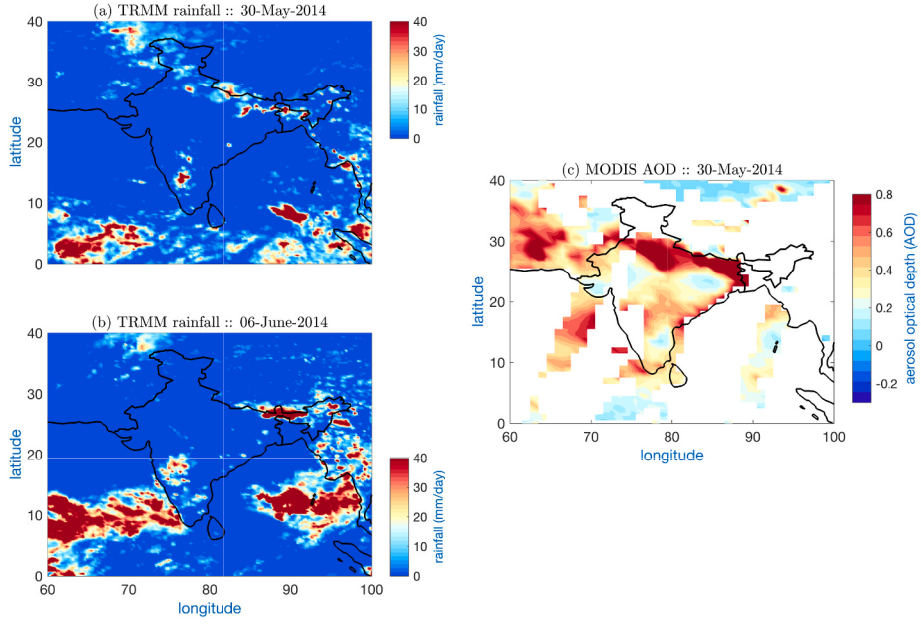

Fig. 2. TRMM rainfall distribution (**a**) on the day of dust storm, (**b**) on the onset of monsoon over Kerala, and (**c**) MODIS aerosol optical depth (AOD) on the day of dust storm. The day of dust storm date is 30*th* May 2014 and the date of onset of monsoon over Kerala is on 6*th* June 2014. Rainfall unit is in mm/day.

model simulation period, i.e., May 27*th* to June 30*th*, 2014. We set up the model for hourly simulation; the regional climate modeling community also recommends validating the model with the same category (ERA data in our case) of the datasets. At the same time, the question on the ERA5 rainfall agreement with the observational pattern is well justified by Hassler and Lauer (2021). Therefore, the model simulated daily average rainfall (mm/day) is validated with the daily averaged ERA5 rainfall (mm/day) (Fig. 3). A rainfall band extending from the Arabian Sea to the Northeastern region through the Indian Ocean and BoB in the ERA5 data (Fig. 3a) is very well captured by the RegCM4.7 simulated rainfall (Fig. 3b). The model simulated rainfall also captures the rainfall pattern over eastern and northeastern India. Fig. 3c represents the bias skill score of the model simulated rainfall distribution computed concerning the ERA pattern. The hatch areas represent the area of significance with a 99% confidence level. The figure shows that East India underestimates the rainfall simulation over the area. The wide areas of northeast India and the southern region of India overestimate the rainfall. Rainfall distribution in the RegCM simulated rainfall over the coastal region of the east, south-east, Coromandel, and western ghat along with Kerala are in agreement with the observation pattern with a high significance level and supported by the previous study by Bhatla et al. (2016). However, the mid-BoB, lower Arabian Sea regions, and the Indian Ocean region show overestimation, and the data distribution meets the significance level. The CC between the reanalysis and model simulated rainfall is presented in Fig. 3d with a 99% confidence level. The spatial CC distribution over the Arabian Sea, Western Ghat, Kerala, and BoB are showingshow good agreement with observation by representing the spatial CC pattern of 0.5 over the regions with a high confidence level. The areas of the Arabian Sea show a highly significant CC of more than 0.6.

For the monsoon advance over the Indian landmass, Kerala, BoB, and the IGP regions have the utmost importance for rainfall propagation. To ensure the model efficiency over those regions, the model output is validated with the observation using some statistical scores. The CC, RMSE, MAE, and FB are calculated using the magic toolbox and placed in Table 1. From the table, it is found that the CC over Kerala is 0.32. In the spatial distribution (refer to Fig. 3d for the spatial CC pattern) over the Kerala region, CC is > 0.4 with a 99% significant level and adds extra

Table 1
CC of BoB and Indian region from IO using the TRMM and model simulated rainfall during the matching period.

	Kerala	BoB	IGP
CC	0.32	0.59	0.51
RMSE	0.41	0.50	0.18
MAE	0.34	0.31	0.12
FB	−0.88	0.61	0.54

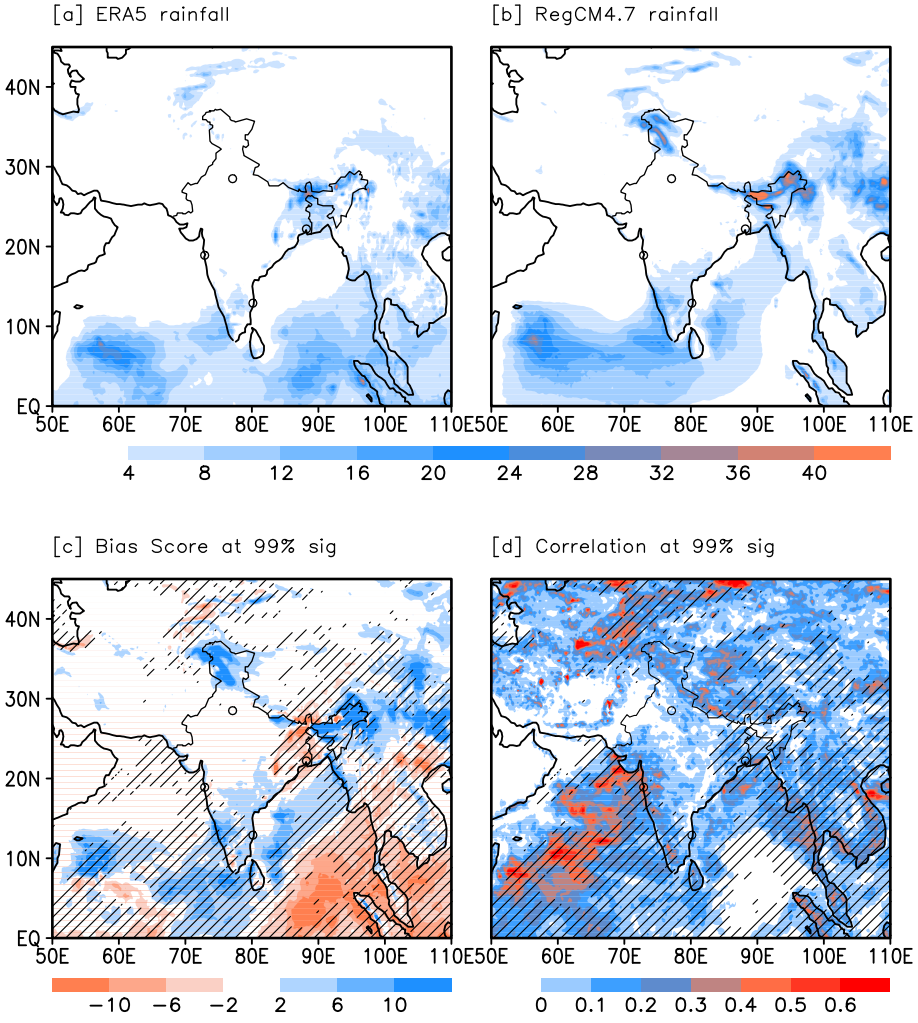

Fig. 3. (**a**) Observational rainfall (ERA5) and (**b**) model simulated rainfall pattern from May 27*th* to June 30*th* of 2014. (**c**) represents the bias skill score between the observation and model simulated rainfall distribution. (**d**) The Correlation Coefficient (CC) between the observation and model data simulation. The hatch represents the area of significance at 99% confidence level. Units are in mm/day.

weightage. Model performance in computing the CC over the BoB is 0.59 with a high confidence level. The spatial pattern over the BoB shows a CC of more than 0.6 with a 99% confidence level. CC over IGP also agrees with the observation by showing a CC of 0.51. RMSE is another widely used error report method in climatology, regression analysis, and forecasting. It ranges from 0 to ∞. A value of 0 indicates a perfect fit of the model data with the observation. Our studies found that the IGP region is a good fit for the observation by showing a 0.18 RMSE value compared to Kerala (0.41) and BoB (0.50). But the RegCM4.7 simulated RMSE is quite good compared to the other regional models (Maharana and Dimri, 2014; Mishra et al., 2020b). MAE is an important statistic used to measure average error. A value close to 0 shows high efficiency in the model performance. The usual MAE pattern shows less MAE over central India than in Kerala and BoB. The present study follows the region-wise MAE pattern by indicating a minimum error of 0.34 (mm/day) over the Kerala and BoB regions and 0.12 (mm/day) over the IGP. FB is dimensionless because of the normalized value of bias. Value varies between +2 and − 2, and the score with 0 is treated as an ideal model performance. The FB measures a good agreement for the IGP region (FB: 0.54) and BoB region (0.61) compared to the Kerala region (FB: −0.88), which shows a slightly high FB with a negative sign. The analysis indicates that RegCM4.7 is very flexible over the ocean by showing a high SD over the region and a good agreement with the ERA5 over the Indian landmass. Model efficiency is also noticeable when performed over the IGP region and performed well over the BoB and Kerala.

3.3. *Model fidelity in capturing the pre-monsoon to monsoon onset rainfall, and the pre-monsoon dust storm*

The model fidelity in capturing the rainfall distribution can be seen in Fig. 4, where the spatial rainfall pattern during the day of the dust storm is placed in Fig. 4a. The model simulated rainfall pattern on the onset of the monsoon can be observed in Fig. 4b. The model simulated pattern can be compared with the TRMM rainfall simulation for those mentioned date from Fig. 2a-b. It is found that the model simulation shows an overestimation over the Kerala region on the day of a dust storm. However, we can ignore this rainfall overestimation after looking at the rain band pattern over the Arabian Sea, which is essential to estimate the propagation of the monsoon onset over Kerala when compared with the TRMM rain band on May 30*th* (Fig. 4a & Fig. 2a). Later, on the day of onset, model simulated onset rainband over the Arabian Sea can grab the reader's attention by successfully simulating the band as of TRMM rainband pattern (Fig. 4b & Fig. 2b). From the figure it can conclude that before the onset and on the day of the dust storm the Arabian Sea experiences the rainfall which is far from the Indian subcontinent. Further, this rainband propagated to the Indian land and hit Kerala on monsoon onset.

The spatial distribution of the dust aerosol over the SA-CORDEX domain on the day of the dust storm is placed in Fig. 5, where Fig. 5a represents the MODIS dust aerosol distribution on 30*th* May 2014 at 10:30 AM. The pattern of the AOD dust plume concentration over north India, centered at Delhi (e.g., Chakravarty et al., 2021), is well captured in model simulated AOD (shaded in Fig. 5b). To make the consistency in the model data distribution with the MODIS AOD pattern, the model AOD is masked over the MODIS grid. The model simulation makes the dust concentration over Delhi and its surrounding regions noticeable. According to the previous studies (e.g., Lau et al., 2006; Lau and Kim, 2006; Vinoj et al., 2014) it has been established that monsoon propagation gets altered due to pre-monsoon dust-storms and it is remote dust. In our study, we have also found the strong signature of it. This remote dust carried from the Arabian desert in middle east Asia uses the possible trajectory over the top of the Arabian Sea. A brief description can be seen in (Vinoj et al., 2014) and explained in section 3e. This remote dust storm needs to be high intensity to reach Indo Gangetic Plain and then AOD gets higher due to coating of anthropogenic pollution. The added value by incorporating the dust model in the model ICBC can be seen in Fig. 5c. The added value in the dust-forced simulation is considered by considering the difference from the without dust-forcing ICBC. The degree of model improvement in simulating AOD can be observed by analyzing the underestimation in AOD value over the IGP (∼ -0.15), Delhi (∼ -0.3), and northwest regions (> -0.3) of India on the day of the dust storm. The model simulated AOD over Delhi (brown line) is further compared with the AERONET station AOD over Jaipur (bin with coral color; Rajasthan state) and Kanpur (bin with sky blue; Uttar Pradesh state) (Fig. 5d). Figure shows the formation of the dust storm by increasing the AOD concentration before the day of the dust storm. It is found that the dust storm over the northern part (specifically over Delhi) lasted for two consecutive days, and the model successfully captured

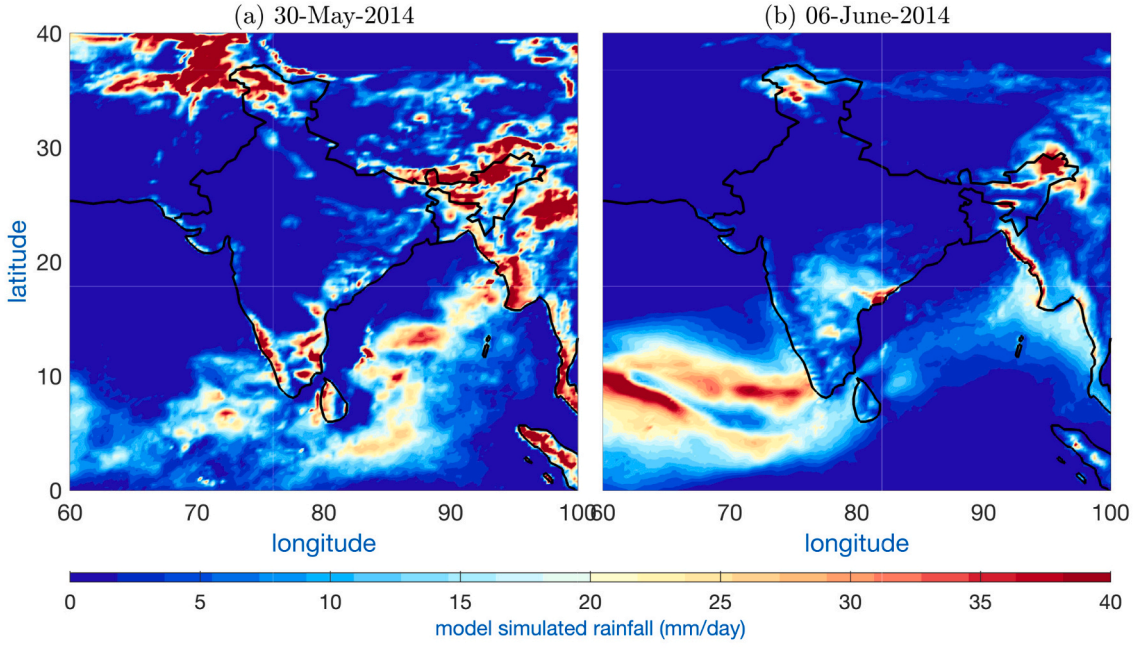

Fig. 4. Similar to Fig. 2a-b but with RegCM4.7 simulated rainfall. Unit is in mm/day.

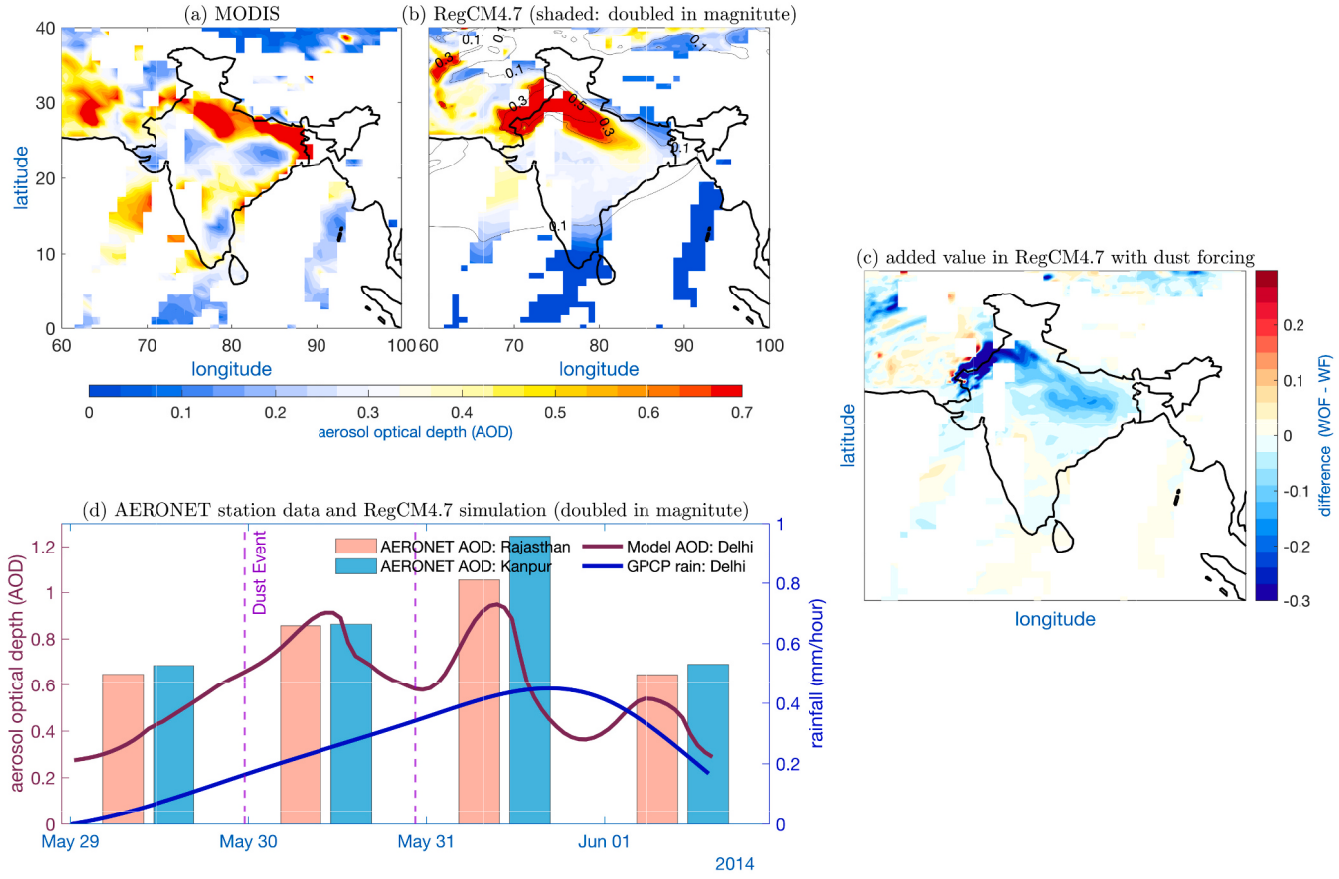

Fig. 5. (**a**) MODIS aerosol optical depth (AOD) (replicating Fig. 2c) and (**b**) simulated AOD distribution from the model on May 30*th*, 2014. Panel **b** is masked on the MODIS satellite pattern where contours depict the actual model-simulated AOD values, with shading representing a doubled magnitude. (**c**) The added value in RegCM4.7 post the incorporation of the dust module. (**d**) AERONET station AOD in Jaipur (represented by coral-colored bins; Rajasthan state) and Kanpur (shown by sky blue bins; Uttar Pradesh state), model-simulated AOD in Delhi (indicated by the brown line), and GPCP rainfall in Delhi (illustrated by the blue line). (For interpretation of the references to color in this figure legend, the reader is referred to the web version of this article.)

both days of the storm. We have provided the observed AOD from AERONET and MODIS, and model simulated AOD to support our findings. The GPCP rainfall over the Delhi region is also considered to see which of the AOD peaks has more impact on monsoon onset propagation. It is found that the dust aerosol dust lasts for 2 consecutive days over Delhi, but the impact of the second-day aerosol is not as impactful as that of the first-day storm. During the second day, the comparatively heavy rain over the Delhi region forced the dust to stagnate.

The analysis shows that the band of highly concentrated AOD regions is spread over the IGP to the NW region of India and the surrounding region of Pakistan. The MODIS TERRA and AQUA maximum AOD patterns also show a similar pattern (Fig. 3; Sethi et al., 2021). On that particular day, AOD over Delhi and its surrounding region triggered the highest value of 1.0 (e.g., Chakravarty et al., 2021). Sethi et al. (2021) show that the Delhi region's primary source of dust concentration is linked with the Thar desert in the NW part of India. According to MODIS satellite data, the areas of middle east Asia were experiencing heavy dust loading. Transmission can also be found from the middle east to the Indian subcontinent through the Arabian Sea. The dust concentration over the IGP region is noticeable as the region experiences a severe dust storm. The signal of the dust aerosol transport from middle east Asia to the Indian subcontinent through the Arabian Sea is visible in the model simulated AOD. However, the dust loading over the region is weaker than the observational pattern (contours in Fig. 5b). The model-simulated AOD is doubled during the data analysis to find the observation AOD pattern and strength. Previous studies by Adebiyi and Kok (2020) have experienced a similar issue when they dealt with the climate model and suggested possible treatments to overcome the model inaccuracy by improving the concentration of coarse minerals dust. They further explain that most climate models lack to capture most of the coarse mineral dust load with a diameter equal to or more than 5 μm in the atmosphere compared to the real world. However, their study suggests the underestimation is 4 times in the model simulation compared to the observation pattern, and we found an improvement by showing the underestimation of 2 times. We considered the dust model by Alfaro et al. (1998) and Zakey et al. (2006) into the model, which deals with the size of mineral dust and the spatial structure of the source region in the model to deal with the specific issue. The present study experienced that doubling the model simulated dust concentration closely matches the MODIS and AERONET AOD pattern as the RegCM4.7 model is limited from the real dust into the model hydrostatic. And because of the presence of natural dust in the model's initial condition, this regional climate model has less compensation for capturing the dust storm over north India. In other words, our study shows an improvement in the model simulation when considering the dust load in the hydrostatic model by capturing the observation pattern by doubling the AOD. We, further seek more attention to the modeler group by highlighting this improvement and forthcoming effort.

The underestimation in the model simulated AOD further motivates us to see its impact on the cloud-precipitation distribution modulated by

aerosol coarse dust deposition. It is tried to convey that during the analysis doubling the model simulated dust concentration closely matches the MODIS and AERONET AOD pattern as the RegCM4.7 model is limited from the real dust into the model hydrostatic. And this regional climate model compensates for capturing the dust storm over north India (contours in Fig. 5b). The underestimation in AOD simulation is very common in most climate models compared to the observation-based AOD, and Adebiyi and Kok (2020) explained the reason very well in their recently published article. In model AOD underestimation, the model tends to deposit the coarse dust out of the atmosphere quickly, causing an important effect on the atmosphere by dust deposition into the ecosystem. The climate model misses the coarse dust equal to or larger than 5 μm in the atmosphere. They further explained that this coarse dust disposition increases the top of the atmosphere coarse dust warming by 0.10 to 0.24 W m^{-2} and affects the cloud and rainfall distribution over the area. To understand this relation between coarse dust decomposition on precipitation, the rainfall simulations are considered with two different conditions (Fig. 6). Fig. 6a is with no dust forcing, and Fig. 6b is with dust forcing in the model simulation. An improvement is noticed in the model simulated rainfall when the dust module is forced into the model (Fig. 6c). The effect of coarse dust decomposition and the increase of dust warming at the mid-troposphere (refer to section 3e for detailed discussion) affects the precipitation distribution and resulting improvement by minimizing the rainfall bias over the Arabian Sea and Kerala coast compared to the rainfall pattern distribution with no force. Our motivation for this study is to see the propagation of monsoon onset and the rainfall over the Kerala coast in response to the dust storm. Therefore, data from the Kerala region is much more important than the rest of India to understand the before and after the monsoon onset propagation. Further, we consider only the positive anomalies $>$ 2 mm/day as both datasets overestimated the Kerala coast during pre- and post-monsoon onset. The result shows the improvement in the RegCM4.7 rainfall simulation over the Arabian Sea rainband region when considering the dust bin in the model's initial condition.

3.4. *Dust loading and transport to the Indian subcontinent and mid-tropospheric synoptic changes*

An attempt is made to understand the changes in the synoptic pattern before and on the day of the dust storm using some meteorological parameters, e.g., Temperature (T), mean sea level pressure (MSLP), and wind, to understand the possible source of dust and the tropospheric changes due to the dust storm (Fig. 7). From the Fig. 7(a1-a2), a temperature gradient is observed over the IGP, NW India, Pakistan, and the middle east. The noticeable temperature variation is observed in the 25–30°N, where a deep temperature gradient is concentrated in west Pakistan and the lower part of Afghanistan and Iran on the previous day of the dust storm (Fig. 7 a1). The monsoon trough region is found at 1000 hPa or more. On the day of the dust storm over Delhi, the concentrated temperature gradient is shifted towards upper central Pakistan and its surrounding regions (Fig. 7 a2). The increase in the temperature gradient over the surface is also noticed over the IGP and central India. The pressure belt (995 hPa) is decreased over the region and IGP. A dry, humid region is simultaneously noted over the high-temperature area, which becomes dryer over 25–35°N (Fig. 7 b1-b2). Delhi and surrounding regions (75–80°E) comparatively experience high temperatures and dry RH over the surface where the RH is 20–40%. The low-level jet (LLJ) is strengthened enough because of the hot and dry conditions over the region. High temperature makes the IGP and surrounding region dry, which drags the wind from the Arabian region and the Arabian Sea towards the northwest part of the Indian region, where the strength of the LLJ at 20–30°N helps to drive the loaded dust to the Indian subcontinent. The hot and dry surface condition supports to rise dust loaded warm air upwards and creates a favorable condition for transporting dust-loaded air parcels far away from their origin. A weak LLJ is experienced over the western ghat and the Arabian Sea before and on the day of the dust storm which could be one of the possible causes of monsoon delay over Kerala.

The dry condition over middle east Asia is triggering the dust loading over the region, and the wind carried the loaded dust to the NW part of India. To understand the mechanism behind the dust loading and transport, the vertical profile of the RH and wind is considered before and on the day of the storm (Fig. 7 c1-c2). The vertical profile of the RH and wind is considered over 40–80°E and averaged over 25–30°N, which is known as a very prominent dust-loaded region to the troposphere (Lau and Kim, 2006). At a lower level (1000–800 hPa), the RH over the Arabian Sea is forcing the loaded dust to be saturated over the sea, and very few loaded dusts in the atmosphere can reach the Indian subcontinent through the lower-level transmission. But the climatic condition (low RH) over 50–70°E in the mid to the upper level shows relatively dry at 600–300 hPa, and over 60–80°E in the lower level (1000–700 hPa) makes the favorable condition to the wind to transmit the loaded dust to the Indian subcontinent on the day of a dust storm (Fig. 7 c1). The high temperature in the atmosphere and less moisture together trigger the wind circulation to carry the loaded dust through middle east Asia (Lau et al., 2006). The dust is loaded with the rising branch of wind, which covers a vast region of 40–70°E and contributes to the dust storm over NW India (e.g., Lau and Kim, 2006), especially over Delhi with a geographical region of 28.70°N and 77.10°E. Lau et al.

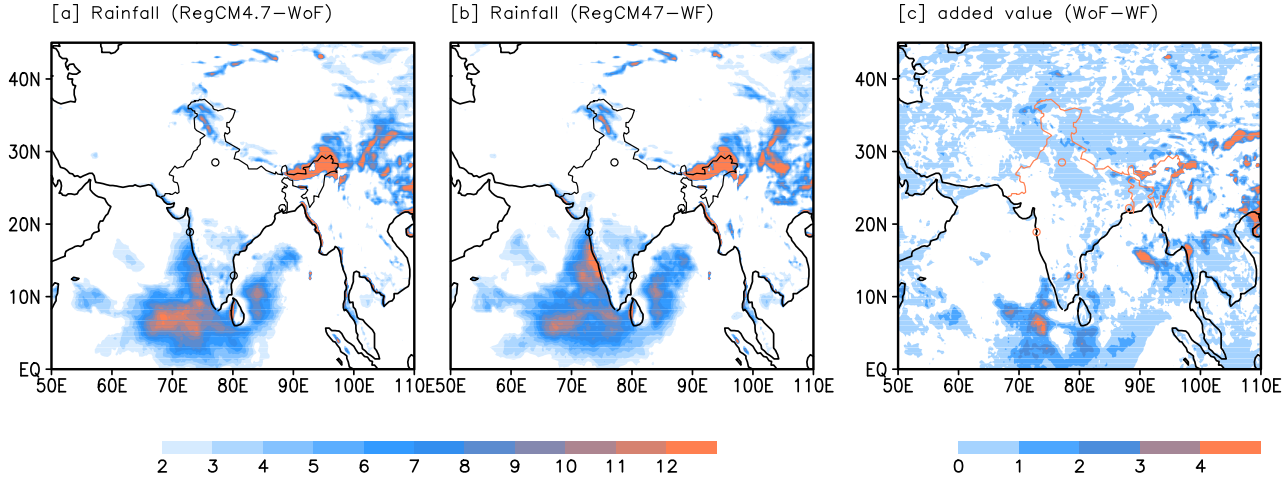

Fig. 6. RegCM4.7 simulated rainfall anomalies from the ERA5 rainfall (**a**) without the dust forcing and (**b**) with dust forcing during the period May 27*th*, 2014 to June 30*th*, 2014, and (**c**) shows the added value in the RegCM4.7 simulated rainfall after considering the dust bin in the model hydrostatics.

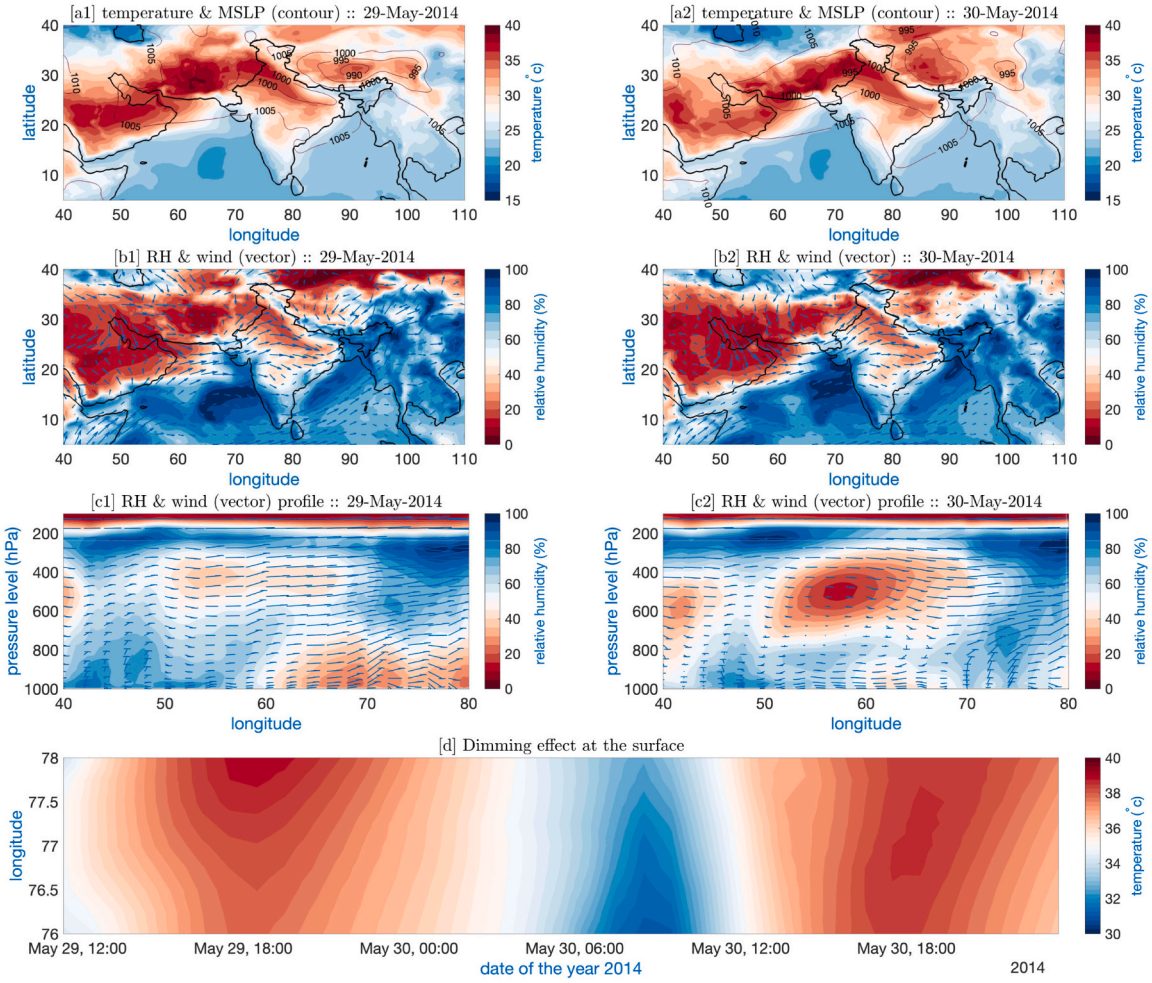

Fig. 7. The spatial distribution and vertical profile of RegCM4.7 simulated temperature (T; unit in °C), MSLP (unit in hPa), RH (unit in %) and wind (m s^{-1}) on the previous day and the day of dust storm i.e., May 29*th*–30*th*, 2014. (**a1-a2**) Spatial pattern during the pre-monsoon T at 925 hPa (shaded with color) where the MSLP is contoured and (**b1-b2**) is the RH at 925 hPa (shaded) with the superimposed wind vector at the same level. (**c1-c2**) represents the vertical profile latitudinal RH (shaded) and the wind profile averaged over 25°N-30°N. (**d**) Decrease in surface temperature due to the dimming effect over Delhi.

(2006) explain that the dust-cloud-radiation-precipitation-circulation at the lower level due to the increase in dust emission and transport over the desert region from middle east Asia resulted in a colder surface in the seasonal time scale. At the same time, the enhanced cloudiness over Pakistan and NW India resulting a warmer and moist atmosphere in the troposphere. On the day of the dust storm, there was a massive change in the vertical wind circulation and the RH pattern (Fig. 7 c2). The mid-upper tropospheric region (700–300) over 50–70°E significantly becomes dryer, and the formation of the western disturbance is noticed over 45–65°E. However, the highly loaded moisture from the Arabian Sea transmits through the lower-level wind to the northwest and southern peninsula and flashes as rain over the Gujarat coast and south India region. The wind, which blows over the southern peninsula, crosses the BoB and reaches the east upper IGP region through the head of BoB and Bangladesh with loaded moisture from the BoB. This transmitted moisture further saturates the dust over the eastern IGP region.

The status of the sudden temperature drop at the surface can be seen in Fig. 7d. This sudden temperature drops over the Delhi region due to the dimming effect is well presented in the RegCM4.7 simulation. It happens when the aerosol particle absorbs the upcoming solar energy and reflects it back into the atmosphere, reducing the direct irradiance of solar energy (Ramanathan et al., 2005; Julsrud et al., 2022). Because of the dust aerosol storm during the daytime over Delhi, the direct irradiance of solar energy is reflected back to space, resulting in the surface cooling from early morning to mid-day on May 30th. The above explanation concludes a well-simulated of the dimming effect by the model and supports the aerosol dynamics for this study.

3.5. *Perturbation of the vertical profile atmospheric heat gradient after the dust storm*

Further, we focus on the mechanism behind the faster propagation of the monsoon onset advance. We consider studying the vertical profile of the ($\frac{\partial \overline{T}}{\partial \phi}$) and the RH pattern. To understand the mechanism, the daily $\frac{\partial \overline{T}}{\partial \phi}$ profile is considered in Fig. 8 from the day of the dust storm to the day of monsoon onset over Kerala. The presented data is zonally averaged over 61°E - 75°E, where *phi* is the latitudinal variation of the respective parameter. The panel shows that the surface temperature over 25–28°N was relatively high on the previous day of the dust event centred over 27.8°N at 925 hPa. The upper atmospheric temperature gradient is somewhat less above the 100 hPa on the very same day. The gradient which connects the surface and upper tropospheric heat by creating a gradient band between 27 and 28°N is much prominent on the day of the dust storm i.e., on 30*th* May. With the progression of time, the surface becomes cooler and the upper troposphere becomes warmer. In the mid of the time frame between the dust event and the monsoon onset, i.e., 1*st* June, the temperature gradient at the mid of the troposphere is noticeable. A positive concentrated temperature gradient is formed in the mid

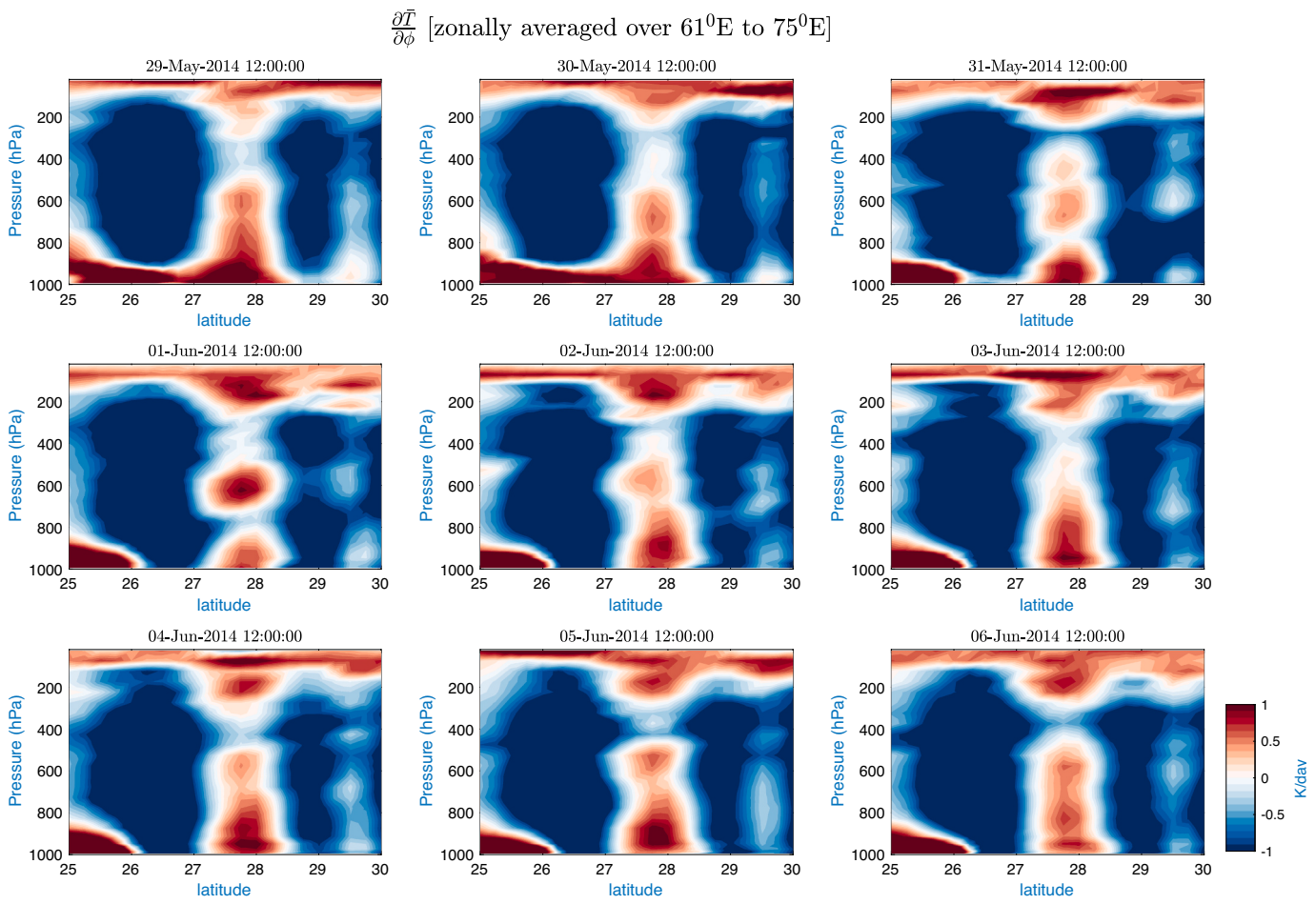

Fig. 8. Model simulated longitudinal heat gradient ($\frac{\partial \bar{T}}{\partial \phi}$) is considered for previous day of the dust event i.e., May 29*th* to the date of onset over Kerala i.e., June 6*th* of 2014. The data is zonally averaged over 61°E to 75°E prepared in a daily time step. An overbar denotes the zonal average. Unit is in K day^{-1}.

troposphere. The upper troposphere gradient is also significantly warmer at the same time, which is the most favorable condition for the dry atmosphere. This dry atmospheric condition, and high temperature gradient over the mid and the upper troposphere together trigger the surface pressure belt towards shrinking over the region. However, the atmosphere maintains the warm condition in the upper troposphere until the onset date and makes suitable conditions for a faster drop in the pressure gradient (refer to Fig. 11b-c) and faster advance the onset towards the Indian subcontinent.

3.6. Position of Western disturbances in the model simulation

To verify the moisture content and the position of the western disturbance in the atmosphere on which the advance of faster movement of onset relies, the vertical profile of RH is investigated after the day of the dust event till the previous day of monsoon onset over Kerala (Fig. 9). The thermodynamic condition on the day of the dust event supports the dust storm over the lower troposphere by maintaining the RH level <40%. A dry condition over the mid-troposphere and the wind strength and direction together make a favorable condition for the transportation of dust from middle east Asia to the NW region of India (refer to Fig. 7 c1-c2). The very next day after the dust storm, when the upper troposphere starts warming, the mid-troposphere's dry condition starts disappearing. The changes in the wind pattern are visible. A wind circulation in the vertical plane sets in with the rising branch over 40°N and shrinking branch over 60–65°N, which is expanded from the lower to the mid of the troposphere. This passage of western disturbances during the end of May caused a delay in establishing the usual pattern of the Heat Low. However, it delayed the monsoon onset for the particular year (IMD Met. Monograph by Pai and Bhan, 2014). With the increasing time and setup of the Heat Low at the mid and upper troposphere, the dry condition becomes prominent in the middle of the troposphere. The wind is strengthened enough with the dry condition increase, and the wind cell's expansion is also noticeable over the surface to the mid-upper troposphere. The increase in the heat gradient over the upper troposphere drags the wind upward and makes it dry, further strengthening the wind circulation by creating a deep dry atmosphere over the mid-troposphere. On the day when the middle of the troposphere experienced the maximum heat gradient (Fig. 8; i.e., June 1*st*), the dry condition covers the whole troposphere over 52–70°N centered over the middle of the troposphere. On June 2*nd*, the dry condition strengthened over the mid-troposphere. The wind at the upper atmosphere starts pushing it to the Indian subcontinent and taking away the gradient at the lower atmosphere from the Indian region. On the 3*rd* and 4*th* of June, the dry state is noticeable and tilted completely. The wind circulation is expanded up to the upper troposphere by widening its circulation at 70–75°N. These changes in the upper to lower troposphere makes the monsoon progression favorable and faster over the Indian subcontinent. The circulation moves westward with time. Further, it can be concluded that this version of the regional climate model efficiently captures the western disturbance over a small scale and subsequently supports the effect of western disturbance after the dust storm and during the advance of monsoon onset.

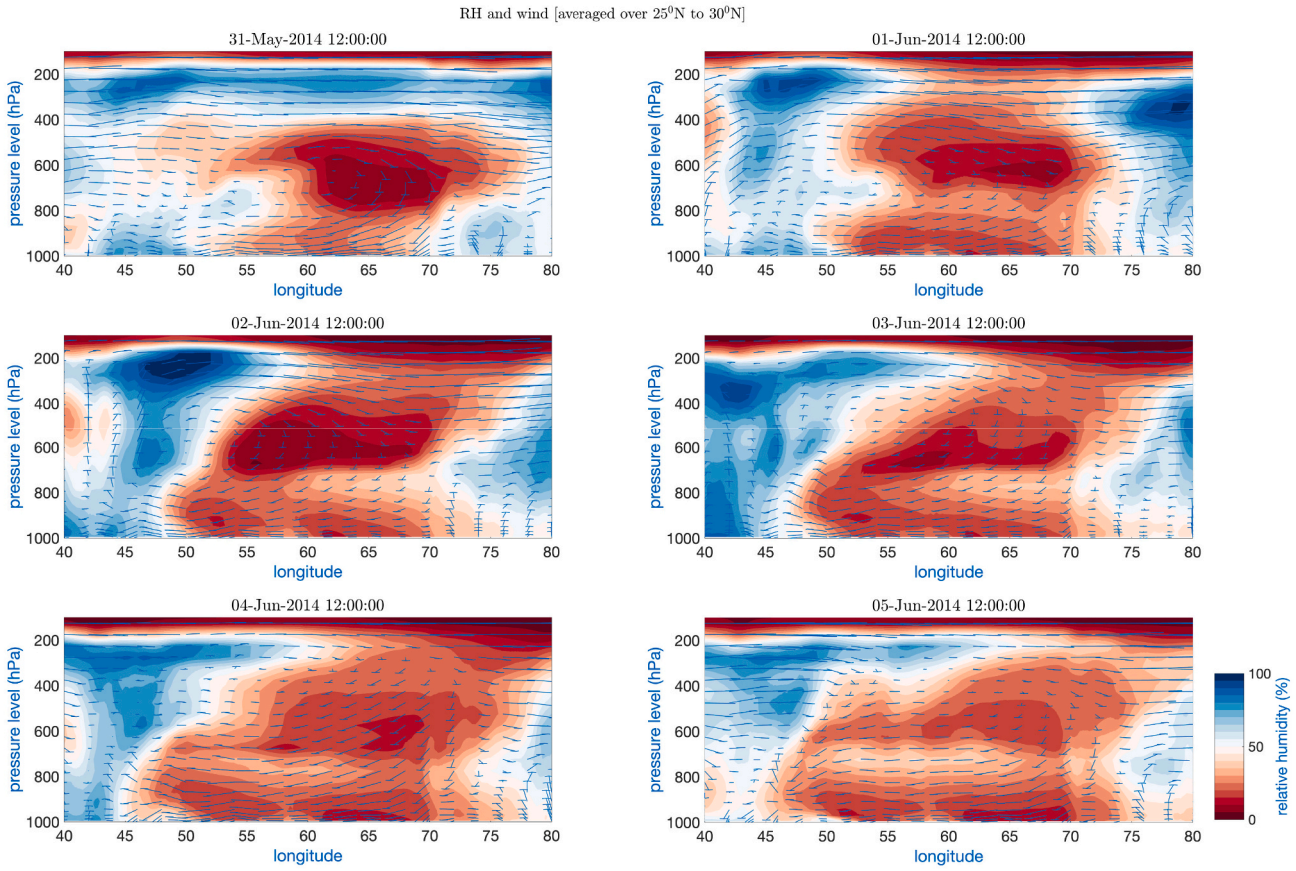

Fig. 9. The latitudinal vertical profile of the RH (shaded) and wind (U and omega in vector), considered after the day of the dust event to the previous day of monsoon onset over Indian region. The data is averaged over 25°N to 30°N on a daily time step. Omega is multiplied with 10^{+5} to understand the vertical effect.

3.7. Progress of regional component of the Hadley cell (RCHC) with the advance of monsoon onset

The strength and position of the regional component of the Hadley cell (RCHC) over the tropics are important in establishing the monsoon condition (e.g., Ghosh et al., 2023). The information regarding the strengthening of the ITCZ and RCHC is shown in Fig. 10. To understand the position of the RCHC over south Asia, the Zonal mean zonal wind and meridional mass stream function is considered over 10°S-40°N and averaged over 70–110°E. The figure distinctly shows that the RCHC is fragile before and on the day of the dust storm (i.e., 29 & 30*th* May). The ascending and descending branch of the RCHC is relatively weak during the days. The wind speed near 850 hPa is also very weak (<5 Knots). A change in the circulation pattern can be noticed after the day of the dust storm (on and after May 31*st*). The ascending and descending branch of the RCHC starts strengthening. With the advance of monsoon onset towards the Indian subcontinent, the ITCZ and the RCHC become intense over the Indian subcontinent (e.g., Joseph et al., 2003). The RCHC shows the highest strength on the day of the monsoon onset over the Indian region (June 6*th*). The westerly also shows its strength at 850 hPa by making the favorable condition for the monsoon onset.

3.8. Formation of the low-pressure belt after the pre-monsoon dust storm

The advance of monsoon is another vital part, and the story of how the AOD induces the monsoon propagation over the Indian subcontinent is described in this section. Several shreds of evidence indicate the monsoon propagation induced by the AOD (Lau et al., 2006; Koren et al., 2012; Vinoj et al., 2014). The study shows that the onset hit Kerala on June 6*th*, 2014, and the above discussion briefly analyzed the monsoon propagation induced by the dust aerosol. Here, we look at how the MSLP changes its pattern after the dust storm and makes a suitable condition before monsoon onset (Fig. 11). Fig. 11a represents the pattern of AOD before and after the dust event and the onset of monsoon rainfall pattern over Kerala and the top of the BoB before and after the onset. The Bin with coral and sky-blue color represents the AERONET station AOD over Jaipur (Rajasthan state) and Kanpur (Uttar Pradesh state), and the brown color line represents the model simulated AOD over Delhi. It can be noticed that the AOD is minimal from 28 to 29*th* May and increase in magnitude on 30*th* May. The capital of India, Delhi, experienced a dust Storm on 30*th* May, and the peak in the AOD pattern is visible and lasts for 2 consecutive days. After the 31*st* of May, it starts decreasing, and this while mechanism is well captured in the model simulation. The solid blue line shows the model-simulated rainfall over Kerala, and the dashed blue line represents the model-simulated onset of monsoon over BoB. The rainfall simulation shows a peak in rainfall estimation over Kerala on June 6*th* (solid blue line) and a peak over BoB on June 8*th*, just after two days of monsoon onset over Kerala. The MSLP over the monsoon trough region was found to fall the same day after the dust event (Fig. 11b-c). The decreasing pattern in the MSLP continued, and the lowest MSLP was reached after a week of the dust event. After two days of dust event, the temperature increased, and the low-pressure belt became stable and reached 995 hPa by June 5*th*. The sudden rise of temperature at the middle and upper troposphere over the NW India region triggers the formation of the low-pressure belt. The heat over the middle and upper troposphere is strongly regulated by the strong north-south thermal gradient and absorption of solar radiation of the elevated dust aerosols over the Arabian Sea, which further escalates the south-

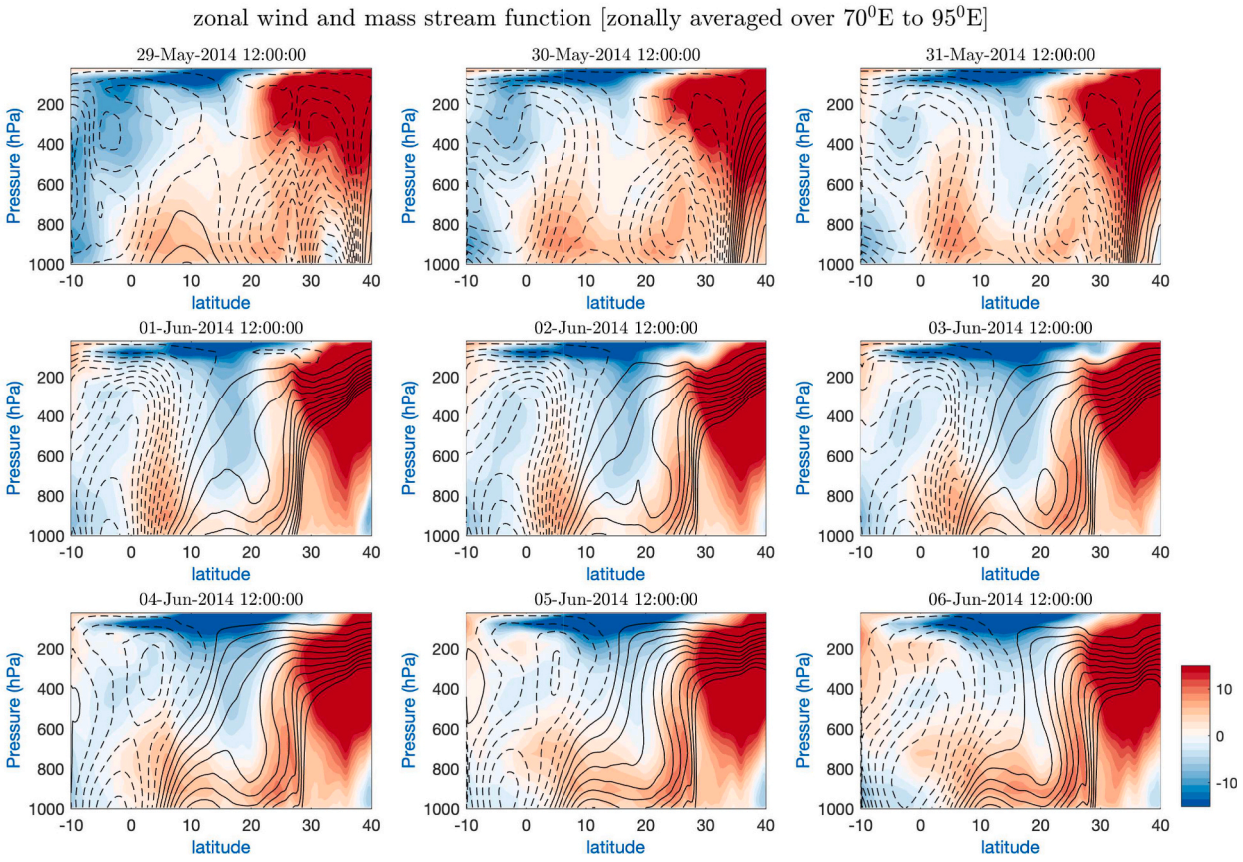

Fig. 10. Zonal mean zonal wind (shaded) and meridional mass stream function (contours; solid line represents positive, and the dashed line represents the negative values) to understand the strength of the meridional wind and the position and strength of the regional component of the Hadley cell (RCHC) before and after the dust storm. The model simulated RegCM4.7 data is averaged over the 70–110°E considering the mentioned parameters. The data is prepared for the daily time step.

westerly jet by transporting loaded moisture from the Arabian Sea to the subcontinent (Jin et al., 2021). At the same time, the Upper Indian region became dry and established a perfect condition for onset over Kerala. The very next day, i.e., June 6*th*, the monsoon hit the Indian landmass (Fig. 11a). The extreme dry condition over the monsoon trough region and the low-pressure belt together boosts the monsoon progress through the top of the BoB to the IGP region.

After monsoon onset over Kerala, onset hits the BoB within two days, i.e., June 8*th*. The area-average rainfall peaks over the BoB for the next consecutive days, along with the development of rainfall peaks (advance of monsoon) over the BoB region, is the witness behind the monsoon advance. The monsoon usually takes about seven days to propagate from Kerala to the head of BoB, and in the year 2014, this propagation from Kerala to the BoB took only two days, much less than its usual time. The dust aerosol loading over the desert plays a semi-direct radiative effect by resulting in a warmer middle and lower troposphere, causing local atmospheric stability and increasing the north-south thermal gradient between the desert region and the Arabian Sea and ending up by enhancing the moisture transport to the Indian subcontinent from the sea (Wang et al., 2021). The intense heat gradient due to the dust storm creates an identical low trough over NW India and IGP that triggers the advance of monsoon over the Indian region.

4. Conclusions

An attempt has been made to understand RegCM4.7 performance to simulate extreme dust events and understand the dust storm's role in ISM onset propagation. The CLM4.5 land surface scheme is compiled in the version of RegCM4.7 where the EIN75 ICBC is forced for the hourly short-time simulation. The RegCM4.7 shows higher performance over the IGP region, including Delhi, for dust storm simulation and overall efficiency in simulating the monsoon onset over the BoB and Kerala. The main findings of the study are as follows:

1. The dust aerosol transport from the middle east of Asia to the northwest (NW) Indian region is prominent during the pre-monsoon dust aerosol storm. A sudden rise in the surface temperature over the northwest region amplifies the elevated heat pump mechanism, loads enough dust for the dust storm over north India, and further triggers a low-pressure belt over the monsoon trough region.
2. The sudden rise in the mid-tropospheric heat gradient after the dust storm adds a positive sense to the warmer condition. It fasts the movement of the monsoon onset, which sets the appropriate weather condition for monsoon onset to advance from the Arabian Sea to the Kerala coast. The formation of the monsoon trough over the Indo-Gangetic Plain (IGP) pulls the moisture-loaded wind towards the Indian subcontinent and provides enough moisture for the onset condition. The additional warm state activates the climatic condition by strengthening the wind, making the atmosphere dry, and forcing the ITCZ and regional component of the Hadley cell (RCHC) to strengthen and shift towards the Indian subcontinent, resulting in faster propagation of the monsoon onset to the Kerala coast.
3. The current version of the regional climate model simulates the formation and propagation of the western disturbances in the upper atmosphere and northern part of India. It can explain possible

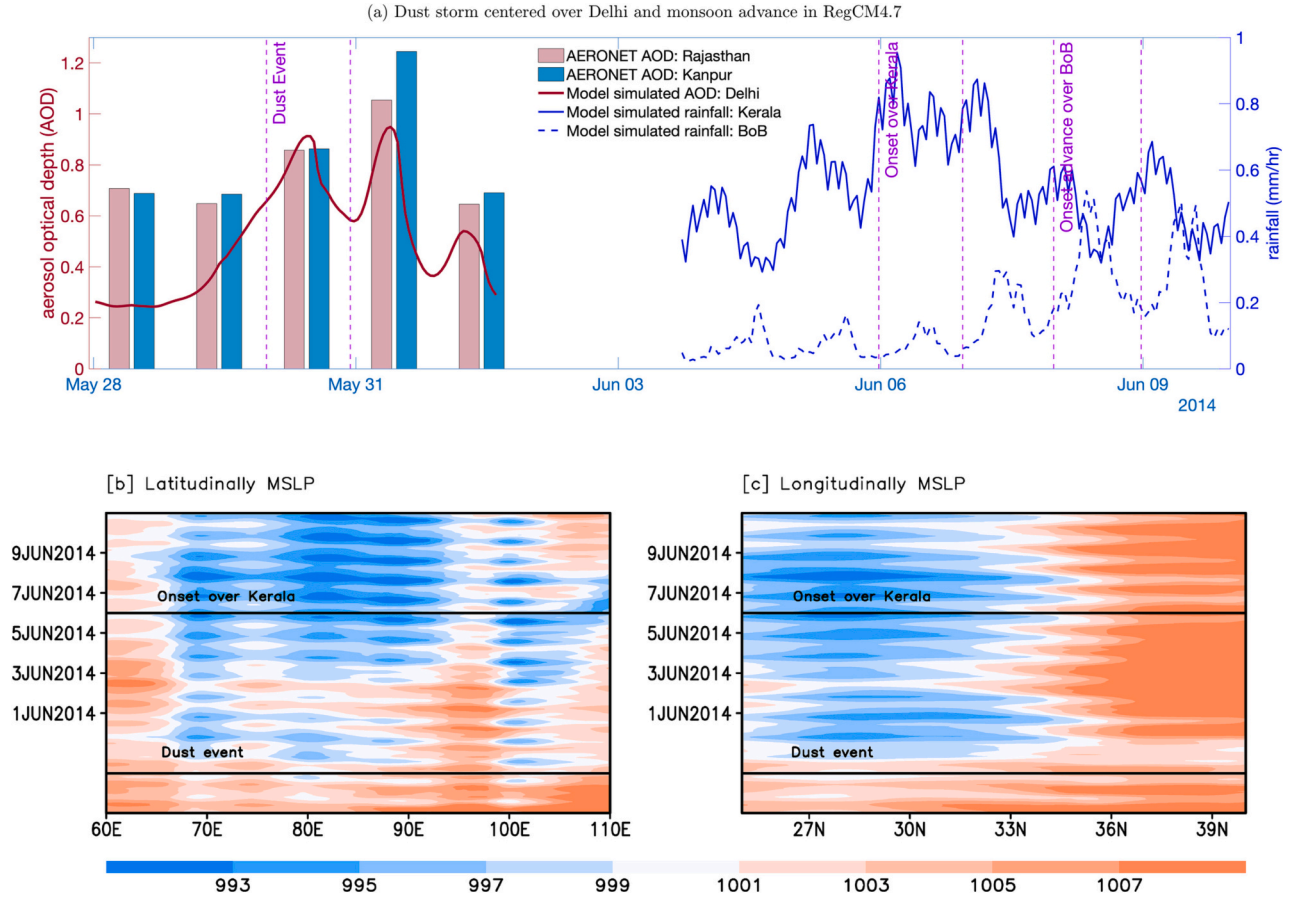

Fig. 11. (**a**) Synoptic pattern of the aerosol optical depth (AOD) over North India and the Indian summer monsoon onset rainfall over Kerala and BoB. Bin with coral and sky-blue color represents the AERONET station AOD over Jaipur (Rajasthan state) and Kanpur (Uttar Pradesh state), and the brown color line represents the model simulated AOD over Delhi. The model simulated AOD is doubled in magnitude. The lines in blue color represents the model simulated rainfall over Kerala and BoB. (**b**) Latitudinal (centered at 27°N) and (**c**) longitudinal (centered at 70°E) MSLP pattern in RegCM4.7. The line series uses hourly datasets whereas the spatial pattern of MSLP uses daily data derived from hourly datasets. (For interpretation of the references to color in this figure legend, the reader is referred to the web version of this article.)

dynamics before and after the dust event over Delhi and adjoint dynamics of monsoon onset faster progress.

4. In 2014, onset hit the Indian subcontinent on June 6th, and further, the monsoon progressed faster than usual and hit the head of BoB within two days. The sudden rise of heat gradient over the mid-troposphere sets the intense low-pressure belt over the monsoon trough region by setting the surface condition warm and dry, and fasts monsoon progress over the IO to the BoB. Because of the faster monsoon propagation from the IO to BoB, the delayed onset propagation recovers the deferred period, and the IGP region experiences on-time monsoon onset.
5. However, the previous studies suggest an underestimation of 4 times the dust load in the model simulation compared to the real atmosphere; we found an improvement by noticing the depreciation of 2 times when considering the dust load in the model. Incorporating the dust model deals with the size of mineral dust and the spatial structure of the source region in the model and leads to a possible reason behind the improvement. Further, the remaining limitation behind the doubling is seeking the community's attention for future improvement.

Open research section

The model code is available at https://github.com/ICTP/RegCM/releases

CRediT authorship contribution statement

Soumik Ghosh: Conceptualization, Data curation, Formal analysis, Investigation, Software, Validation, Visualization, Methodology, Writing - original draft. **Abhijit Sarkar:** Formal analysis, Investigation, Methodology, Validation, Writing – review & editing. **R. Bhatla:** Formal analysis, Funding acquisition, Resources, Supervision. **R.K. Mall:** Funding acquisition, Resources, Supervision. **Swagata Payra:** Conceptualization, Formal analysis, Investigation, Methodology, Supervision, Validation, Writing – review & editing. **Priyanshu Gupta:** Data curation, Software, Visualization.

Declaration of Competing Interest

The authors declare that they have no known competing financial interests or personal relationships that could have appeared to influence the work reported in this paper.

All the authors have accepted the author's sequence and declared no conflict of interest.

Data availability

Data will be made available on request.

Acknowledgments

This research is partially supported by a grant from the Department of Science and Technology (DST), Govt. of India under FIST Program - 2022 (SR/FST/ES-1/2022/102). The authors express their gratitude to the diligent efforts of the two anonymous reviewers, whose insightful feedback significantly enhanced the caliber of this manuscript. SG wishes to acknowledge Dr. Manish Soni for invaluable assistance in configuring the HPC environment for model installation. The authors also extend their appreciation to Dr. Pramod Kumar for providing the Fortran code of the magic toolbox. Furthermore, acknowledgment is extended to ICTP for making available the RegCM4.7 code, and to NASA for granting access to the MODIS AOD, AERONET AOD, GPCP, and TRMM rainfall datasets. All authors have unanimously agreed on the sequence of authors and have declared no conflicts of interest.

References

Adebiyi, A.A., Kok, J.F., 2020. Climate models miss most of the coarse dust in the atmosphere. Sci. Adv. 6, eaaz9507.
Alfaro, S.C., Gaudichet, A., Gomes, L., Maillé, M., 1998. Mineral aerosol production by wind erosion: aerosol particle sizes and binding energies. Geophys. Res. Lett. 25, 991–994.
Bhatla, R., Ghosh, S., Mandal, B., Mall, R., Sharma, K., 2016. Simulation of indian summer monsoon onset with different parameterization convection schemes of regcm-4.3. Atmos. Res. 176, 10–18.
Bhatla, R., Verma, S., Ghosh, S., Mall, R., 2020. Performance of regional climate model in simulating indian summer monsoon over indian homogeneous region. Theor. Appl. Climatol. 139, 1121–1135.
Bollasina, M.A., Ming, Y., Ramaswamy, V., 2011. Anthropogenic aerosols and the weakening of the south asian summer monsoon. Science 334, 502–505.
Bretherton, C.S., Peters, M.E., Back, L.E., 2004. Relationships between water vapor path and precipitation over the tropical oceans. J. Clim. 17, 1517–1528.
Chakravarty, K., Vincent, V., Vellore, R., Srivastava, A., Rastogi, A., Soni, V., 2021. Revisiting andhi in northern India: a case study of severe dust-storm over the urban megacity of New Delhi. Urban Clim. 37, 100825.
Das, S., Dey, S., Dash, S., Basil, G., 2013. Examining mineral dust transport over the indian subcontinent using the regional climate model, regcm4. 1. Atmos. Res. 134, 64–76.
Das, S., Dey, S., Dash, S., 2016. Direct radiative effects of anthropogenic aerosols on indian summer monsoon circulation. Theor. Appl. Climatol. 124, 629–639.
Dee, D.P., Uppala, S.M., Simmons, A.J., Berrisford, P., Poli, P., Kobayashi, S., Andrae, U., Balmaseda, M., Balsamo, G., Bauer, D.P., et al., 2011. The era-interim reanalysis: Configuration and performance of the data assimilation system. Q. J. R. Meteorol. Soc. 137, 553–597.
Elguindi, N., Bi, X., Giorgi, F., Nagarajan, B., Pal, J., Solmon, F., Giuliani, G., 2013. Regional climate model regcm user manual version 4.4. In: The Abdus Salam International Centre for Theoretical Physics, Strada Costiera, Trieste, Italy, vol. October 21, p. 54.
Emanuel, K.A., Živković-Rothman, M., 1999. Development and evaluation of a convection scheme for use in climate models. J. Atmos. Sci. 56, 1766–1782.
Ganguly, D., Rasch, P.J., Wang, H., Yoon, J.H., 2012. Climate response of the south asian monsoon system to anthropogenic aerosols. J. Geophys. Res.-Atmos. 117.
Ghosh, S., Bhatla, R., Mall, R., Srivastava, P.K., Sahai, A., 2019. Aspect of ecmwf downscaled regional climate modeling in simulating indian summer monsoon rainfall and dependencies on lateral boundary conditions. Theor. Appl. Climatol. 135, 1559–1581.
Ghosh, S., Sinha, P., Bhatla, R., Mall, R., Sarkar, A., 2022. Assessment of lead-lag and spatial changes in simulating different epochs of the indian summer monsoon using regcm4. Atmos. Res. 265, 105892.
Ghosh, S., Miller, A.J., Subramaniam, A.C., Bhatla, R., Das, S., 2023. Signals of northward propagating monsoon intraseasonal oscillations (misos) in the regcm4. 7 cordex-core simulation over south asia domain. Clim. Dyn. 1–15.
Giorgi, F., Coppola, E., Solmon, F., Mariotti, L., Sylla, M., Bi, X., Elguindi, N., Diro, G., Nair, V., Giuliani, G., et al., 2012. Regcm4: model description and preliminary tests over multiple cordex domains. Clim. Res. 52, 7–29.
Grell, G.A., Dudhia, J., Stauffer, D.R., et al., 1994. A Description of the Fifth-Generation Penn State/NCAR Mesoscale Model (MM5). Mesoscale and Microscale Meteorology Division, National Center for ….
Hassler, B., Lauer, A., 2021. Comparison of reanalysis and observational precipitation datasets including era5 and wfde5. Atmosphere 12, 1462.
Hersbach, H., Bell, B., Berrisford, P., Hirahara, S., Horányi, A., Muñoz-Sabater, J., Nicolas, J., Peubey, C., Radu, R., Schepers, D., et al., 2020. The era5 global reanalysis. Q. J. R. Meteorol. Soc. 146, 1999–2049.
Heymsfield, A.J., McFarquhar, G.M., 2001. Microphysics of indoex clean and polluted trade cumulus clouds. J. Geophys. Res.-Atmos. 106, 28653–28673.
Jiang, Y., Liu, X., Yang, X.Q., Wang, M., 2013. A numerical study of the effect of different aerosol types on east asian summer clouds and precipitation. Atmos. Environ. 70, 51–63.
Jin, Q., Wei, J., Lau, W.K., Pu, B., Wang, C., 2021. Interactions of asian mineral dust with indian summer monsoon: recent advances and challenges. Earth Sci. Rev. 215, 103562.
Joseph, P., Sooraj, K., Rajan, C., 2003. Conditions leading to monsoon onset over Kerala and the associated hadley cell. Mausam 54, 155–164.
Julsrud, I.R., Storelvmo, T., Schulz, M., Moseid, K.O., Wild, M., 2022. Disentangling aerosol and cloud effects on dimming and brightening in observations and cmip6. J. Geophys. Res.-Atmos. 127 e2021JD035476.
Kiehl, J., Hack, J., Bonan, G., Boville, B., Briegleb, B., 1996. Description of the NCAR Community Climate Model (CCM3). Technical Note. National Center for Atmospheric Research, Boulder, CO (United States …).
Konwar, M., Parekh, A., Goswami, B., 2012. Dynamics of east-west asymmetry of indian summer monsoon rainfall trends in recent decades. Geophys. Res. Lett. 39.
Koren, I., Altaratz, O., Remer, L.A., Feingold, G., Martins, J.V., Heiblum, R.H., 2012. Aerosol-induced intensification of rain from the tropics to the mid-latitudes. Nat. Geosci. 5, 118–122.
Kosmopoulos, P., Kaskaoutis, D., Nastos, P., Kambezidis, H., 2008. Seasonal variation of columnar aerosol optical properties over Athens, Greece, based on modis data. Remote Sens. Environ. 112, 2354–2366.
Krishnamurti, T., Martin, A., Krishnamurti, R., Simon, A., Thomas, A., Kumar, V., 2013. Impacts of enhanced ccn on the organization of convection and recent reduced counts of monsoon depressions. Clim. Dyn. 41, 117–134.
Lau, K.M., Kim, K.M., 2006. Observational relationships between aerosol and asian monsoon rainfall, and circulation. Geophys. Res. Lett. 33.
Lau, K., Kim, M., Kim, K., 2006. Asian summer monsoon anomalies induced by aerosol direct forcing: the role of the tibetan plateau. Clim. Dyn. 26, 855–864.
Lohmann, U., Feichter, J., 2005. Global indirect aerosol effects: a review. Atmos. Chem. Phys. 5, 715–737.
Maharana, P., Dimri, A., 2014. Study of seasonal climatology and interannual variability over India and its subregions using a regional climate model (regcm3). J. Earth Syst. Sci. 123, 1147–1169.
Maharana, P., Dimri, A., 2016. Study of intraseasonal variability of indian summer monsoon using a regional climate model. Clim. Dyn. 46, 1043–1064.
Maharana, P., Dimri, A., Choudhary, A., 2019. Redistribution of indian summer monsoon by dust aerosol forcing. Meteorol. Appl. 26, 584–596.
Manoj, M., Devara, P., Safai, P., Goswami, B., 2011. Absorbing aerosols facilitate transition of indian monsoon breaks to active spells. Clim. Dyn. 37, 2181–2198.
Meehl, G.A., Arblaster, J.M., Collins, W.D., 2008. Effects of black carbon aerosols on the indian monsoon. J. Clim. 21, 2869–2882.
Mishra, A.K., Dubey, A.K., 2021. Sensitivity of convective parameterization schemes in regional climate model: precipitation extremes over India. Theor. Appl. Climatol. 146, 293–309.
Mishra, A.K., Dwivedi, S., Das, S., 2020a. Role of arabian sea warming on the indian summer monsoon rainfall in a regional climate model. Int. J. Climatol. 40, 2226–2238.
Mishra, A.K., Dwivedi, S., Di Sante, F., Coppola, E., 2020b. Thermodynamical properties associated with the indian summer monsoon rainfall using a regional climate model. Theor. Appl. Climatol. 141, 587–599.
Nair, V.S., Solmon, F., Giorgi, F., Mariotti, L., Babu, S.S., Moorthy, K.K., 2012. Simulation of south asian aerosols for regional climate studies. J. Geophys. Res.-Atmos. 117.
Nober, F.J., Graf, H.F., Rosenfeld, D., 2003. Sensitivity of the global circulation to the suppression of precipitation by anthropogenic aerosols. Glob. Planet. Chang. 37, 57–80.
Oleson, K., Lawrence, D., Bonan, G., Drewniak, B., Huang, M., Koven, C., Levis, S., Li, F., Riley, W., Subin, Z., et al., 2013. Technical Description of Version 4.5 of the Community Land Model (Clm)(no. ncar/tn-503+ str). UCAR, Boulder, CO, USA.
Ongoma, V., Tabari, H., 2023. Climate Impacts on Extreme Weather: Current to Future Changes on a Local to Global Scale. Elsevier Science.
Pai, D., Bhan, S., 2014. Monsoon 2013. National Climate Centre (NCC), India Meteorological Department (IMD). Govt. of India.
Pal, J.S., Small, E.E., Eltahir, E.A., 2000. Simulation of regional-scale water and energy budgets: Representation of subgrid cloud and precipitation processes within regcm. J. Geophys. Res.-Atmos. 105, 29579–29594.
Pant, M., Ghosh, S., Verma, S., Sinha, P., Mall, R., Bhatla, R., 2022. Simulation of an extreme rainfall event over Mumbai using a regional climate model: a case study. Meteorog. Atmos. Phys. 134, 1–17.
Pant, M., Bhatla, R., Ghosh, S., Das, S., Mall, R., 2023. Will warming climate affect the characteristics of summer monsoon rainfall and associated extremes over the gangetic plains in India? Earth and Space Sci. 10 e2022EA002741.
Papadimas, C., Hatzianastassiou, N., Mihalopoulos, N., Querol, X., Vardavas, I., 2008. Spatial and temporal variability in aerosol properties over the mediterranean basin based on 6-year (2000–2006) modis data. J. Geophys. Res.-Atmos. 113.
Parth Sarthi, P., Ghosh, S., Kumar, P., 2015. Possible future projection of indian summer monsoon rainfall (ismr) with the evaluation of model performance in coupled model inter-comparison project phase 5 (cmip5). Glob. Planet. Chang. 129, 92–106.
Parth Sarthi, P., Kumar, P., Ghosh, S., 2016. Possible future rainfall over gangetic plains (gp), India, in multi-model simulations of cmip3 and cmip5. Theor. Appl. Climatol. 124, 691–701.
Ramanathan, V., Chung, C., Kim, D., Bettge, T., Buja, L., Kiehl, J.T., Washington, W.M., Fu, Q., Sikka, D.R., Wild, M., 2005. Atmospheric brown clouds: Impacts on south asian climate and hydrological cycle. Proc. Natl. Acad. Sci. 102, 5326–5333.
Sethi, D., Radhakrishnan, S., Sharma, C., Mishra, S., et al., 2021. Aerosol optical properties over Delhi during a dust event in summer 2014: plausible implications. Indian J. Phys. 95, 2531–2540.
Shahi, N.K., Das, S., Ghosh, S., Maharana, P., Rai, S., 2021. Projected changes in the mean and intra-seasonal variability of the indian summer monsoon in the regcm

cordex-core simulations under higher warming conditions. Clim. Dyn. 57, 1489–1506.
Sinha, P., Mohanty, U., Kar, S., Dash, S., Kumari, S., 2013. Sensitivity of the gcm driven summer monsoon simulations to cumulus parameterization schemes in nested regcm3. Theor. Appl. Climatol. 112, 285–306.
Solmon, F., Giorgi, F., Liousse, C., 2006. Aerosol modelling for regional climate studies: application to anthropogenic particles and evaluation over a european/african domain. Tellus Ser. B Chem. Phys. Meteorol. 58, 51–72.
Solmon, F., Nair, V., Mallet, M., 2015. Increasing arabian dust activity and the indian summer monsoon. Atmos. Chem. Phys. 15, 8051–8064.
Stocker, T., 2014. Climate Change 2013: The Physical Science Basis: Working Group I Contribution to the Fifth Assessment Report of the Intergovernmental Panel on Climate Change. Cambridge University Press.
Tiedtke, M., 1989. A comprehensive mass flux scheme for cumulus parameterization in large-scale models. Mon. Weather Rev. 117, 1779–1800.
Verma, S., Bhatla, R., 2021. Performance of regcm4 for dynamically downscaling of el nino/la nina events during southwest monsoon over India and its regions. Earth and Space Sci. 8 e2020EA001474.
Verma, S., Bhatla, R., Ghosh, S., Sinha, P., Kumar Mall, R., Pant, M., 2021. Spatio-temporal variability of summer monsoon surface air temperature over India and its regions using regional climate model. Int. J. Climatol. 41, 5820–5842.
Verma, S., Bhatla, R., Shahi, N., Mall, R., 2022. Regional modulating behavior of indian summer monsoon rainfall in context of spatio-temporal variation of drought and flood events. Atmos. Res. 274, 106201.
Vinoj, V., Rasch, P.J., Wang, H., Yoon, J.H., Ma, P.L., Landu, K., Singh, B., 2014. Short-term modulation of indian summer monsoon rainfall by west asian dust. Nat. Geosci. 7, 308–313.
Wang, M., Lau, W.K., Wang, J., 2021. Impact of middle east dust on subseasonal-to-seasonal variability of the asian summer monsoon. Clim. Dyn. 57, 37–54.
Zakey, A., Solmon, F., Giorgi, F., 2006. Development and testing of a desert dust module in a regional climate model. Atmosph. Chemi. Phys. Discuss. 6, 1749–1792.
Zeng, X., Zhao, M., Dickinson, R.E., 1998. Intercomparison of bulk aerodynamic algorithms for the computation of sea surface fluxes using toga coare and tao data. J. Clim. 11, 2628–2644.